J. Chem. Eng. Data 1988, 33, 1-5

Complexation and Transport Properties in Binary Glass-Forming Molten Chloride Systems

Anselmo Elias

Department of Chemistry, University of Lisbon, Lisbon, Portugal

C. Austen Angell*

Department of Chemistry, Purdue University, West Lafayette, Indiana 47907

Following a recent study of the contrasting effects of $FeCl_4^-$ versus $CrCl_6^{3-}$ complex anion formation on the transport properties of solutions containing them, we report a study of the intermediate cases of MCl_4^{2-} complex formation ($M = Co^{2+}$, Ni^{2+}, and Cd^{2+}). In these cases an intermediate and unspectacular response is observed, and secondary factors intercede to produce an apparent contradiction between composition-dependent behavior close to, and far from, the glass transition. The contradictions are resolved by recognizing that, in these intermediate cases, the predominant effect of complexation is to produce a decrease in liquid "fragility".

Introduction

In a recent paper, the authors examined the behavior of fluidity and conductance in two binary molten salt systems containing a common monovalent chloride to which was added, alternatively, one of the trivalent chlorides $FeCl_3$ or $CrCl_3$ (*1*). The interest content of this work lay in the fact that, although the trivalent cations are next-to-nearest neighbors in the periodic table, the transport properties, on addition of the trivalent chlorides, changed in opposite directions. The observations were interpreted in terms of the different effects on the liquid cohesion of the formation of octahedral chloro complexes, $CrCl_6^{3-}$, in one case, the tetrahedral chloro complexes, $FeCl_4^-$, in the other. In the present paper we extend this investigation. We examine the fluidity and conductance in two binary systems in which 3d transition-metal tetrahedral chloro complexes carrying double negative charges, $NiCl_4^{2-}$ and $CoCl_4^{2-}$, are known to form. The common component is again the glass-forming organic cation salt α-picolinium chloride (α-methylpyridinium chloride). A third system containing a tetrahedral chloro complex of a 4d transition metal with complete d shell, $CdCl_4^{2-}$, has been included for comparison.

Experimental Section

Materials. α-Picolinium chloride, designated hereafter α-picHCl, was purified by a distillation procedure described elsewhere (*2*); it melted sharply at 91–91.5 °C. The inorganic chlorides $NiCl_2$, $CoCl_2$, and $CdCl_2$ were obtained in pure anhydrous form from Alpha Chemical Co. and were used without further purification.

Binary melts were prepared by fusing the preweighed components under nitrogen and checking for weight loss, all operations being carried out under nitrogen in a drybox atmosphere. The transport properties discussed below were measured immediately after the melt preparation.

Differential scanning calorimetry (DSC) and differential thermal analysis (DTA) were performed, respectively, to determine (a) the phase diagram in the case of the system α-picHCl + $CoCl_2$ system, and (b) the glass transition temperatures of both systems. For DSC studies, samples were hermetically sealed into aluminum pans in the drybox and scanned at 10 °C, using the Perkin-Elmer DSC-1 instrument. Only one scan was performed on each sample to avoid the danger of contamination by the aluminum sample pan once melting had occurred. The T_g values were determined independently by DTA of small samples contained in 4-mm Pyrex tubes scanning at ~8 °C min^{-1}. EMF's were recorded with a Houston X-Y3000 recorder.

Transport Measurements. Kinematic viscosities and electrical conductivities of the three binary chloride systems were determined on the same sample by using the hybrid Ubbelohde capillary viscometer–conductivity cell described by Gammel and Angell (*3*). The cell constant was determined by using standard solutions (1.0 and 0.1 D) of KCl in water at 25 °C, and was found to be 26.82 ± 0.02. The viscometer *C* constant was determined with water and aqueous solutions of sucrose, 30% w/w. The value found was $C = (4.998 \pm 0.0015) \times 10^{-2}$ cSt s^{-1}.

All melts were hot-filtered before admission to the measuring cell, both filtration and cell-filling operations being again conducted in the drybox.

The vertical posture of the viscometry capillary was checked by two spirit levels mounted at right angles at the top of the cell. The same provisions described previously (*1*) for isolating the sample from the external atmosphere while pumping the melt inside the viscometer were used in the present work. The temperature was controlled ±0.1 °C by a photodiode system described elsewhere (*4*). Measurements were conducted between an upper limit imposed by either vaporization of the salt or polymerization of the silicone bath fluid, and a lower limit determined by crystallization of the melt or, when no crystallization occurred, by exceeding the limits of the measuring system. Flow times were measured by a TC-13 Advanced Electronics LTD electronic timer giving a precision of 0.01 in the range 46–20 000 s. The kinetic energy correction was never greater than 0.01% and was ignored. Standard deviations in the time from run to run were always less than 0.15%.

The conductivities were determined with a Wayne-Kerr B641 autobalance universal bridge at 1592 Hz with a nominal accuracy of 0.05%. Fifteen successive measurements of the conductivity were made at each temperature for each sample. Crystallization was detected by a time dependence of the conductivity. Temperature stability likewise could be judged from a time independence of the measurements.

Results

The phase diagram for the system α-picHCl + $CoCl_2$ is shown in the upper part of Figure 1. The highest melting point in the part of the diagram investigated occurs at the stoichiometry of the tetrachloro complex, as is commonly found. The results indicate a further compound at the stoichiometry 1:1, which presumably involves infinite chains of $CoCl_4$ tetrahedra linked through their corners. A further compound is indicated at 20 mol % $CoCl_2$ perhaps analogous to alkali-

0021-9568/88/1733-0001$01.50/0

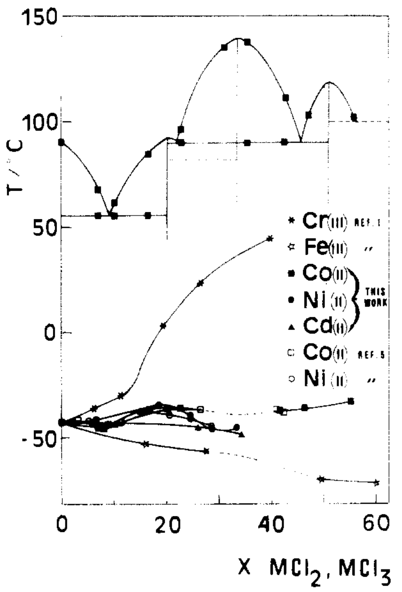

Figure 1. Phase diagram for the system α-picHCl + $CoCl_2$ and glass transition temperatures for various α-picHCl + MCl_2 or MCl_3 systems.

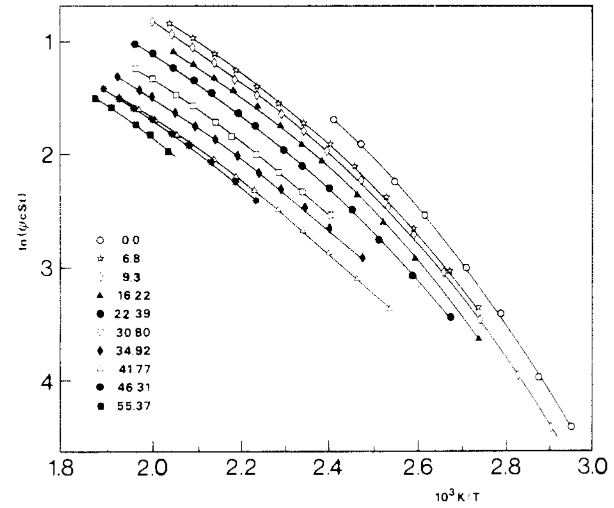

Figure 2. Arrhenius plots of kinematic fluidity for solutions in the system α-picHCl + $CoCl_2$.

metal-rich compounds in the $NiCl_2$–alkali metal chloride systems (*5*), or to the compounds with hydrogen-bonded dications seen in $ZnCl_2$–PyHCl and $AlCl_3$–PyHCl systems (*6–8*). The diagram is essentially a replica of the $ZnCl_2$–PyHCl system in its features.

The behavior of the glass transition temperature in the region investigated is shown in the lower section of Figure 1 where it is compared with the results previously obtained for $CrCl_3$- and $FeCl_3$-containing systems (*1*). We also include the limited data on glass transition temperatures obtained for the systems α-picHCl + $NiCl_2$ and α-picHCl + $CdCl_2$ obtained in the present work.

The initial dip in the glass transition temperatures for the $CoCl_2$-containing system essentially confirms measurements made at more closely spaced intervals in an earlier study by Hodge (*8*). Hodge observed remarkable changes in the intensity of the ligand field spectrum for cobalt in this composition range which to date have remained unexplained. For our purposes it is sufficient to note that this is a region of somewhat complex behavior, and we will seek phenomenological correlations without attempting detailed structural explanations of their origin at this time. We must note, though, that the initial dip in T_g is particularly strange in view of the uncomplicated behavior of the binary system containing $ZnCl_2$, since Co(II) in general follows the behavior of Zn(II) rather closely.

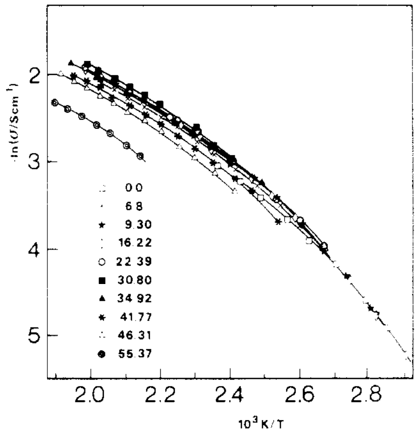

Figure 3. Arrhenius plots of electrical conductivity for solutions in the system α-picHCl + $CoCl_2$.

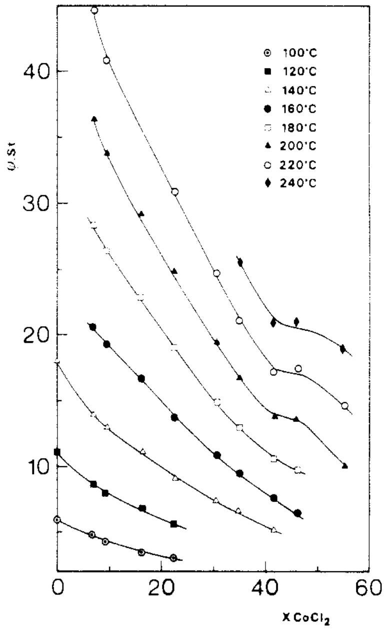

Figure 4. Isothermal plots of fluidity as a function of $CoCl_2$ content in the system α-picHCl + $CoCl_2$.

Turning now to the transport properties, we encounter a series of surprises. Data for the fluidities are shown as Arrhenius plots in Figure 2. The data for pure α-picHCl coincide with those determined in two previous studies within 2%. Addition of $CoCl_2$ causes systematic decreases in the fluidity up to the maximum composition, despite the expectation from the behavior of T_g that there would be an initial increase. Such an increase is, on the other hand, observed in the conductivity, see Figure 3 (also Figure 5 referred to below), though it has almost been removed at the lowest temperatures where one would in principle expect the effect of an initial decrease in T_g to cause the largest increase. The variations with composition are demonstrated more clearly in the isothermal plots of Figures 4 and 5.

The anticorrelation of fluidity and conductance behavior is also seen, though to a lesser degree, in the behavior of the $NiCl_2$-based binary system. The temperature dependences of the different properties are shown in Figures 6 and 7, and the isothermal behavior in Figures 8 and 9. Tables of the data displayed in Figures 2–9 are provided in the microform publication of this work. (See Supplementary Material Available paragraph at the end of this article.)

Transport data for the system α-picHCl + $CdCl_2$ have also been obtained and are available in the microform publication

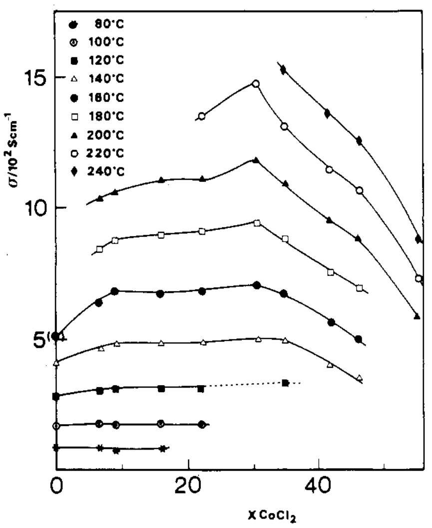

Figure 5. Isothermal plots of electrical conductivity as a function of $CoCl_2$ content in the system α-picHCl + $CoCl_2$.

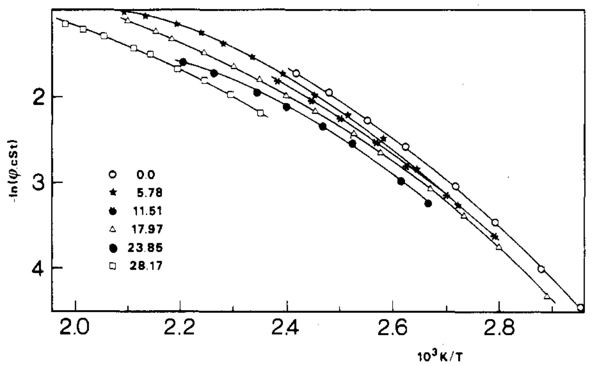

Figure 6. Arrhenius plots of kinematic fluidity for solutions in the system α-picHCl + $NiCl_2$.

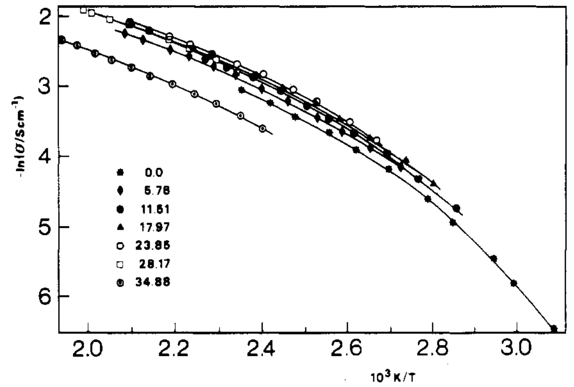

Figure 7. Arrhenius plots of electrical conductivity for solutions in the system α-picHCl + $NiCl_2$.

of this work. They show very similar trends to those of the data in Figures 2–9.

Discussion

The difference between the composition dependence of viscosity at high temperatures (short relaxation times) and at low temperatures (long relaxation times near T_g) pointed out in the previous paragraphs is unusual. Measurements at temperatures closer to T_g will be required before complete explanations can be given. However, the findings could be explained if there is a change in "fragility" (*9*) of the liquid on complexation, such that the complexes liquids are less fragile despite lower T_g values than the parent α-picHCl. A manifestation of decreased fragility is a decrease in the curvature of the Arrhenius plot and this affects the temperature interval above T_g which must be traversed before a given short value of the relaxation time, or low value of viscosity, can be reached. The behavior we observe would then be consistent with the idea explained in detail in ref *9* that fragility is related to the facility with which the molecular order can reorganize, particularly in the intermediate distance range of 10–15 Å. This facility should be impeded by complexation. We come back to this matter and provide supporting evidence later in the discussion.

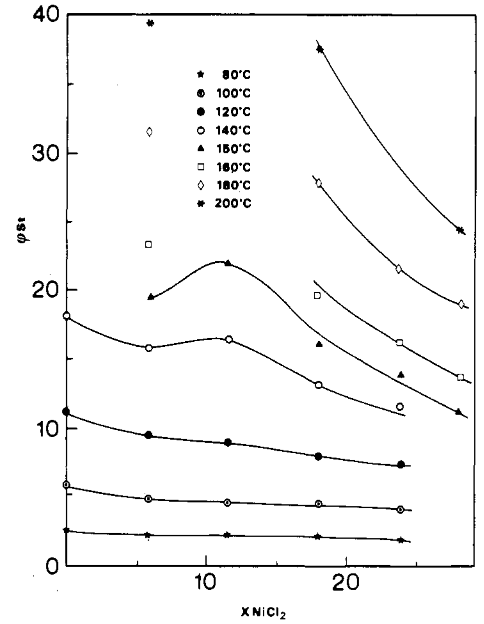

Figure 8. Fluidity isotherms for solutions in the system α-picHCl + $NiCl_2$.

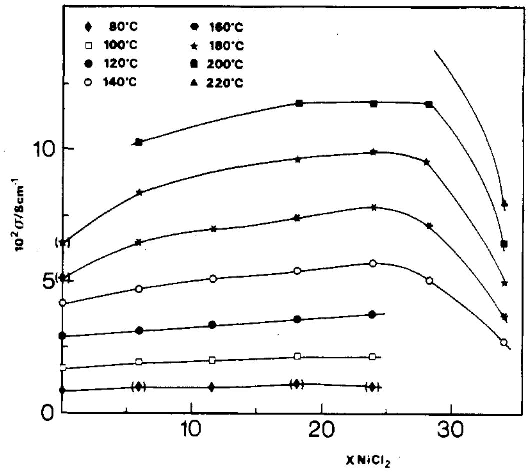

Figure 9. Isothermal plots of electrical conductivity as a function of $NiCl_2$ content in the system α-picHCl + $NiCl_2$.

In the meantime it is helpful to compare the present results with those from the earlier study on systems containing $FeCl_3$ and $CrCl_3$, some data for which are included in Figure 1. It is seen that the behavior in the present system with respect to composition effects is essentially intermediate between that of the previous two systems and this, at least, is naturally interpretable in terms of the intermediate charge density on the complex being produced on solution, ($FeCl_4^-$, $CoCl_4^{2-}$, $CrCl_6^{3-}$).

The distinction between the composition dependence of the fluidity and that of conductivity in both systems is probably to be understood in terms of a decrease in ion pairing due to hydrogen bonding in α-picolinium chloride as the hydrogen bonding power of Cl^- is reduced on complexation. Evidence for

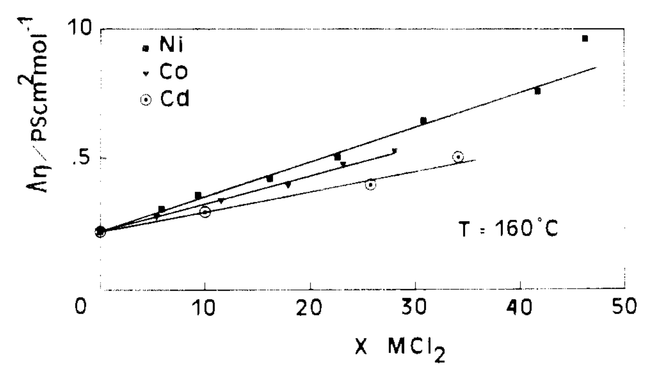

Figure 10. Variation of the Walden product $\Lambda\eta$ with addition of different divalent metal chlorides to α-picHCl.

this effect from NMR studies has been given previously (*9*). It is best demonstrated from the present results by display of the Walden product $\Lambda\eta$, where Λ is the equivalent conductivity and η the viscosity. This product is a constant in "well-behaved" systems in which there is a fixed concentration of charge carriers and in which the retarding forces acting on the charge carriers scale with the viscosity. If anything, this quantity might be expected to decrease on addition of MCl_2 as complexation decreases the concentration of charge carriers. For the present system, however, there are rapid increases, see Figure 10. Although it was not emphasized in our earlier discussion of the trivalent-chloride-based systems (*1*), the same sort of increase in the Walden product occurred in those systems. The difference is that the composition dependence of the transport properties in that case was dominated by the difference in the anion types formed whereas in the present system, in which the latter effect is intermediate, the relative importance of the ion pairing (dissociation) phenomenon is brought out. Similar behavior of the Walden product has been seen in complexing systems of the more common non-glass-forming alkali metal chloride + MCl_2 type (*10*), however, which indicates that the above explanation is only part of a more general phenomenon.

We turn now to the behavior of the glass transition temperatures T_g. In the previous study with trivalent cation second components (*1*), it was demonstrated that the opposite trends observed in T_g with MCl_3 additions could be correlated with the transport properties by fitting the data to the three-parameter Vogel–Tamman–Fulcher (VTF) equation

$$\sigma,\ \phi = A_i \exp[-B_i/(T - T_0)]$$

(where A_i, B_i, and T_0 are constants) and extracting T_0 ($T_0 < T_g$). To obtain systematic behavior of T_0 with composition it was necessary to keep B constant for each property in order to reduce the statistical noise due to measurement imprecision and to the small range of transport coefficients which were explored. In view of the "strong" and "fragile" behavior pattern for glass-forming liquids, in which a common high-temperature extreme for liquid viscosities is indicated (*9*), it would probably be more appropriate in the present case to choose A constant so that variations in fragility (which are related to variations in the B parameter, see below) with composition could be revealed. However, for consistency with the previous article (*1*) we keep B constant and show, in Figure 11, the behavior of the free parameters A and T_0 with composition for the α-picHCl + $CoCl_2$ system. The features to be noted are the correct prediction of the puzzling (and so far unexplained) dip in T_g at small $CoCl_2$ content, and the existence of a weak minimum in T_0 in the vicinity of the expected complex anion stoichiometry, $CoCl_4^{2-}$. A weaker minimum was strongly indicated by direct observations of T_g in the more strongly glass-forming system containing $ZnCl_2$ system (*2*) and would be consistent with a minimum in cohesive energy at this composition (*11*).

Beyond the complex anion stoichiometry, corner linking of the tetrahedral $CoCl_4$ units is to be expected. The increase in intermediate range order associated with this polymerization should produce a decrease in the fragility of the liquid structure, i.e., a decrease in the rate of temperature-induced structural degradation and, according to the recent analysis one of us (*9*), should produce a shift in the reduced Arrhenius plot for viscosity toward the center of the general pattern (see Figure 12). Such a shift is necessary to rationalize the otherwise conflicting T_g and isothermal viscosity composition variations discussed in the opening paragraph of this section. Accordingly, we show the

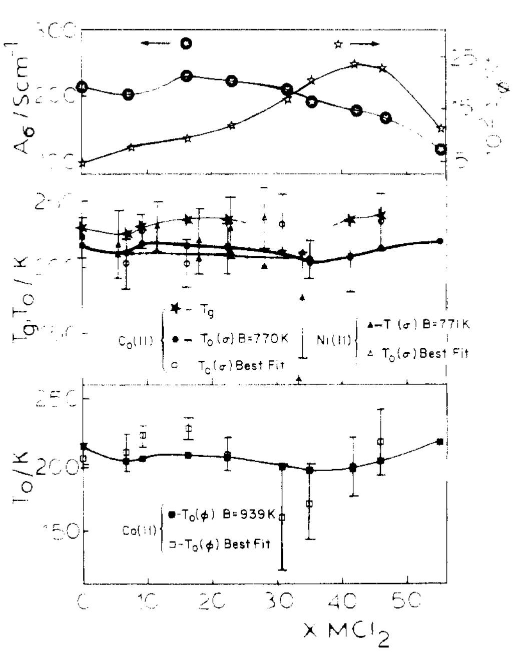

Figure 11. Variation of the free VTF equation parameters, A_ϕ, A_σ, $T_{0,\phi}$, $T_{0,\sigma}$, with composition in the α-picHCl + CCl_2 system. T_g values from Figure 1 have been included for comparison.

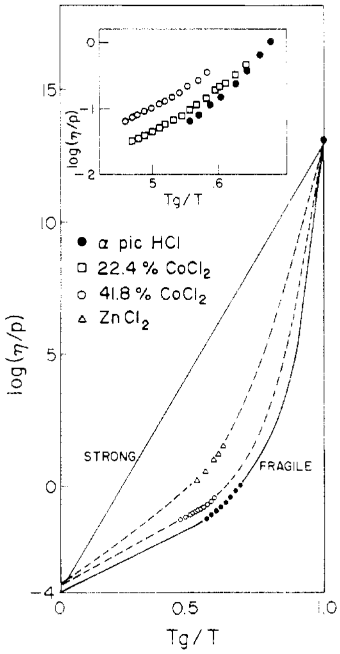

Figure 12. T_g-reduced Arrhenius plot of viscosity for the extreme compositions studied in the α-picHCl + $CoCl_2$ system, compared with data for pure $ZnCl_2$ (to which pure $CoCl_2$ is related in behavior) and to the limiting cases in the general "strong and fragile liquids" pattern (see ref *9*). Insert: detail on the present system.

J. Chem. Eng. Data **1988**, *33*, 5-8

T_g-reduced representation for the α-picHCl + $CoCl_2$ system in Figure 12 insert and see that the expected behavior is realized. The relative fragility of *all* of the liquids of this study can be appreciated from the position of our extreme cases in the overall "strong and fragile liquids" pattern of Figure 12.

Concluding Remarks

This study and its predecessor (*1*) have shown that the consequences, to ion mobility, of complexation processes in ionic liquids, depend on the sort of complex anions which are formed. For fixed charge types, viscosities may increase on complexation if the coordination number in the complex formed is large rather than small (e.g. 6 rather than 4) so that the residual charge on the ligands remains large (e.g., $-^1/_2$ in $CrCl_6^{3-}$ vs $-^1/_4$ in $FeCl_4^-$). This provokes the question of whether similar effects can be seen in the case where the second component cation remains fixed but the coordination number adopted increases due to a smaller ligand size, e.g., NiF_6^{4-} vs $NiCl_4^{2-}$. Experiments designed to test this idea have been carried out and will be reported separately (*12*).

Registry No. α-picHCl, 14401-91-3; $CoCl_2$, 7646-79-9; $NiCl_2$, 7718-54-9; $CdCl_2$, 10108-64-2.

Literature Cited

(1) Angell, C. A.; Elias, A. *J. Phys. Chem.* **1983**, *87*, 4704.
(2) Angell, C. A.; Hodge, I. M.; Cheeseman, P. A. *Molten Salts*; Pensler, J. P., Ed.; The Electrochemical Society: Pennington, NJ, 1976; p 138.
(3) Gammel, P. M.; Angell, C. A. *J. Chem. Phys.* **1974**, *60*, 584.
(4) Elias, A.; Pereira, M. H. *Rev. Port. Quim.* **1973**, *15*, 6.
(5) Smith, G. P. *Molten Salt Chemistry*; Blander, M., Ed.; Interscience: New York, 1964.
(6) Easteal, A. J.; Angell, C. A. *J. Phys. Chem.* **1970**, *74*, 3987.
(7) Angell, C. A.; Shuppert, J. W. *J. Phys. Chem.* **1980**, *84*, 538.
(8) Hodge, I. M. Ph.D. Thesis, Purdue University, 1974.
(9) (a) Angell, C. A. *Relaxations in Complex Systems*; Ngai, K., Wright, G. B., Eds.; National Technical Information Service, U.S. Department of Commerce: Springfield, VA, 1984. (b) Angell, C. A. *J. Non-Cryst. Solids* **1985**, *73*, 1.
(10) Harrap, B. S.; Heymann, E. *Trans Faraday Soc.* **1955**, *51*, 268.
(11) Moynihan, C. T.; Angell, C. A. *Molten Salts*; Mamantov, G., Ed.; Marcel Dekker: New York, 1969; p 315.
(12) Elias, A.; Angell, C. A., to be published.

Received for review July 24, 1986. Revised manuscript received May 22, 1987. Accepted August 10, 1987. We are indebted to the National Science Foundation and the Gulbenkian Foundation for support of this work under Solid State Chemistry Grant No. DMR 8304887.

Supplementary Material Available: Tables of conductivity and kinematic viscosity data for compositions in the three systems of this study [α-picolinium chloride + ($NiCl_2$ or $CoCl_2$ or $CdCl_2$)] (19 pages). Ordering information is given on any current masthead page.

Thermal Conductivities in Seven Ternary Liquid Mixtures at 40 °C and 1 Atm

Richard L. Rowley* and Vernon Gubler

Department of Chemical Engineering, 350 CB, Brigham Young University, Provo, Utah 84602

A transient hot-wire thermal conductivity cell has been used to measure ternary liquid mixture thermal conductivities over the entire composition range at 40 °C and ambient pressure. These data were used to evaluate a previously developed local-composition model for prediction of mixture thermal conductivity. Comparison to the previous results obtained for these systems at 25 °C indicates that, over the small temperature range considered in this work, the local-composition parameters (obtained from the literature from binary vapor–liquid equilibrium) may be considered constant without loss of accuracy.

Introduction

Industrial needs for fluid-mixture thermal conductivity coupled with the variety of mixture compositions and constituencies of possible interest mandates development of an effective multicomponent predictive technique. A local-composition (LC) predictive model for multicomponent thermal conductivity has been reported and tested for binary liquid mixtures (*1*). It is based on the nonrandom two-liquid (NRTL) model (*2*) originally developed for equilibrium properties. As such, the model uses only pure-component thermal conductivities and binary NRTL interaction parameters obtained from vapor–liquid equilibrium (VLE) data of the constituent binary systems. Lack of multicomponent mixture thermal conductivity data has until recently precluded testing of the model for other than binary mixtures.

In order to provide ternary mixture thermal conductivity data against which multicomponent models can be evaluated, we designed and constructed a transient hot-wire thermal conductivity apparatus suitable for accurate measurements of liquid thermal conductivities over a moderate temperature range. The apparatus has been tested and evaluated for pure-component and binary mixture data (*3*). It has also been used to test the efficacy of the LC model for ternary liquid mixtures at 25 °C (*4*). In the latter study, it was found that the model's assumption of binary interactions is adequate and that reasonably accurate predictions can be expected from the model for ternary liquid mixtures with no adjustable parameters. We report here the measurement of ternary mixture thermal conductivities at 40 °C for seven systems. These data indicate that using temperature independent NRTL interactions does not affect the predictions over moderately small temperature ranges.

Experimental Section

The transient hot-wire technique is generally considered to be the most accurate method currently available for measurement of liquid mixture thermal conductivity. It has been employed since the late 1930s and the bulk of the most recent thermal conductivity measurements have been made by this technique. Its history of use, equation derivation, analysis assumptions, experimental techniques, error analysis, assets, and limitations have been carefully studied and are readily available (*5*–*11*).

The thermal conductivity cell used in this work was a single-wire cell, machined from 316 stainless steel and sealed with Viton O-rings. The platinum measurement wire, 0.0005 in. in diameter, was obtained from American Fine Wire Co. with the specifications of 99.95% purity and 266.8 ± 5% Ω/ft. A special cell insert, machined from thin-walled (0.04 inches), 0.50-in.-o.d., stainless steel tubing, was employed to secure and

0021-9568/88/1733-0005$01.50/0 © 1988 American Chemical Society